A W-BAND WAFER PROBE

Edward M. Godshalk

Cascade Microtech, Inc.
Beaverton, Oregon

ABSTRACT

A W-band (75-110 GHz) wafer probe is presented. The probe uses ridge-trough waveguide to transition from a rectangular waveguide input to coplanar waveguide used on the probe board output. Research was conducted on radiation loss and moding in coplanar waveguide to minimize insertion loss and maintain a coplanar mode. The probe is shown to work successfully and data is presented for W-band HEMTs.

I. INTRODUCTION

Microwave and millimeter wave monolithic integrated circuit technology has matured to a high degree under such programs as the DARPA MIMIC effort [1]. The intent of this program is to develop cost effective millimeter wave integrated circuits for such applications as radar front ends for missile seekers and aircraft systems. For any of these applications wafer probes are required for characterization and testing of the circuits while they are still in wafer form. The circuits must be tested at the wafer level, since inserting defective devices into systems typically raises the cost of using monolithic IC's to an unrealistic level. The cutting edge for many applications of monolithics is in the 75-110 GHz region, prompting the development of the W-band wafer probe presented here. The performance of this probe and its application to measuring some W-band devices will also be discussed.

A waveguide to coplanar waveguide (CPW) transition was required to extend the upper frequency limit of wafer probes, since commercially available coaxial cable assemblies overmode above 65 GHz. Such a transition was developed during the construction of a waveguide input wafer probe covering V-band (50-75) GHz. [2]. An operational diagram for a waveguide input wafer probe is shown in Figure 1. A rectangular waveguide input enters a transition section where the dominant TE_{10} mode of the waveguide is converted to a coplanar field pattern. The coplanar mode is then launched on to a CPW transmission line printed on the lower surface of an alumina probe board. At the tip of the probe board a hard metal, such as nickel, is deposited on the CPW metalization to form fingers. These fingers make contact with the device under test (DUT) on the wafer. Typically coplanar pads are formed at the DUT test ports to allow contact with these probe fingers.

DARPA funded the development of the W-band [Army Phase III MIMIC] and V-band [Navy Phase III MIMIC] wafer probes.

The transition for the W-band probe was similar in concept to that developed for the V-band probe, and will be reviewed. Significant research was required to develop a CPW probe board with low insertion loss at W-band and low radiation. Excessive radiation might cause perturbations of measured data due to nearby structures. A successful design was achieved which resulted in the construction of the high performance W-band wafer probes reported here.

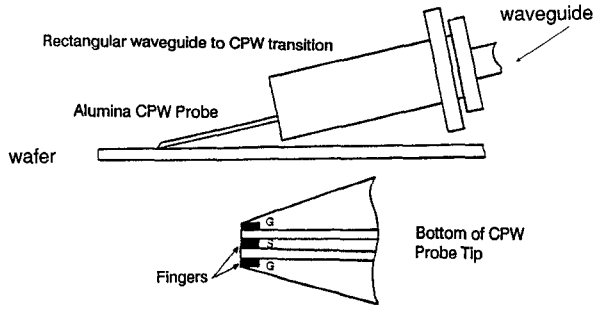

Figure 1. The waveguide input wafer probe.

II. TRANSITION DESIGN

Figure 2 illustrates the transition design in greater detail. The rectangular waveguide input is illustrated in (a), which supports the TE_{10} mode as shown. Next, a ridge is gradually introduced, which forms the quasi-TEM field pattern as in (b). The ridge-trough waveguide is formed by gradually adding a trough below the ridge as shown in (c). By lowering the ridge into the trough, the electric field is split and rotated forming a coplanar field, with a characteristic impedance of 50 ohms in this case. This field pattern is similar to that found in the coplanar waveguide illustrated in (d). The final step is to launch the coplanar mode into a 50-ohm CPW transmission line. The CPW line is inverted, as shown in (e) to bring its grounds into contact with the lower surface of the waveguide. The signal line of the CPW is attached to the ridge with a gold bond ribbon. This completes the transition process.

A test fixture was constructed to evaluate the transition design. For W-band, a WR-10 rectangular waveguide was transitioned to 50-ohm ridge-trough waveguide and then back to WR-10 waveguide. Having rectangular waveguides at each port of the test fixture allowed testing with a HP-8510C waveguide test set for use at W-band. Figure 3 shows the insertion loss (S_{21}) and return loss (S_{11}) of the transition.

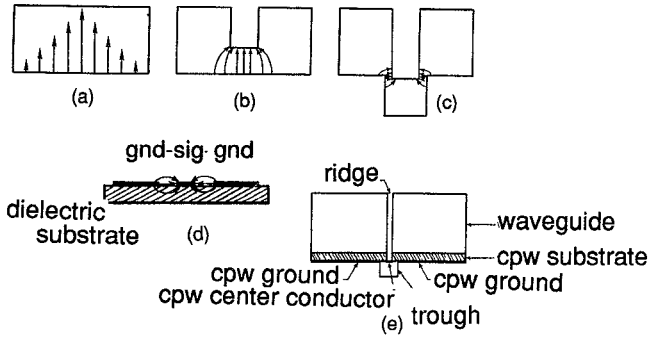

Figure 2. Transition from TE_{10} electric fields to coplanar waveguide type fields.

Since the measured insertion loss is actually for two transitions (i.e. back-to-back), the appropriate scale for S_{21} is approximately half the measured loss to give the effective loss for a single transition. The insertion loss is less than 0.7 dB from 75 to 106.5 GHz rising to 0.8 dB at 110 GHz. The return loss is better than 15 dB over the entire band, except at two spots.

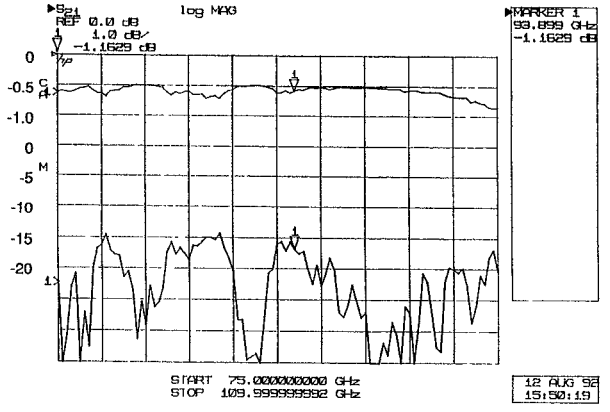

Figure 3. Insertion and return loss for back-to-back rectangular to ridge-trough waveguides.

III. PROBE BOARD RESEARCH

The CPW probe board design presented two primary challenges: low insertion loss, and low crosstalk between probes when two or more probes are in close proximity while probing a device. Insertion loss in CPW transmission lines is generally attributed to radiation loss and conductor loss when low-loss dielectric substrates are used. At the onset of the CPW design, radiation loss was expected to be the dominant insertion loss factor based on prior research [3]. Using a similar approach, the predicted radiation loss was computed for three CPW transmission lines on alumina, having gaps of .001, .002, and .004 inches (G in Figure 4). In each case the signal line width (W) was increased to maintain a 50-ohm characteristic impedance. Figure 5 shows the results, which imply that radiation loss increases with gap size.

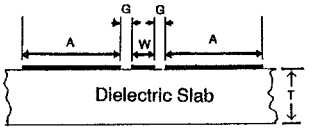

Figure 4. Cross section of a Coplanar Waveguide (CPW).

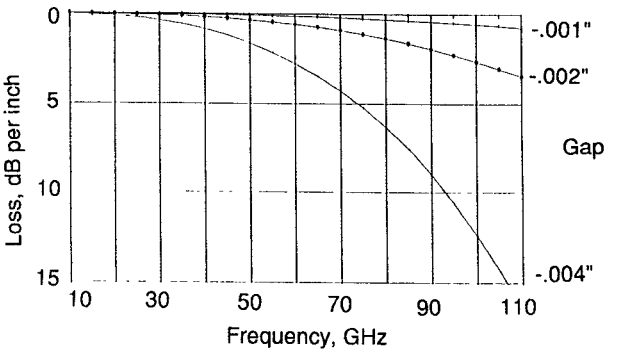

Figure 5. CPW radiation loss vs. frequency for three different gaps.

To verify these predictions a radiation study was conducted. This consisted of measuring the insertion loss (S_{21}) of three coplanar waveguide (CPW) transmission lines, all 1.00 inch long. The three CPW lines differ in gap and signal line dimensions (see Table 1). In each case W and G are chosen for a characteristic impedance of 50 ohms. Figure 6 shows the results, which are opposite of what was predicted. The implication is that radiation loss was negligible and that the signal line width (W) dominates. It is speculated that this dominance is due to the reduction of signal line resistance with increasing width, but further study is recommended to discover why the expected radiation loss is not present. A possible explanation is that the radiation model used does not account for conductor thickness and our gold layer is relatively thick.

Table 1.

Line #	W	G
1	.003"	.002"
2	.008"	.004"
3	.019"	.008"

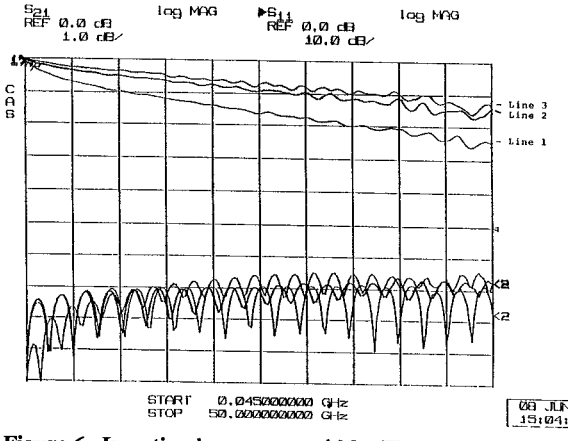

Figure 6. Insertion loss vs. gap width. The gaps are .002", .004", and .008" for lines 1,2, and 3 respectively. All lines have 50 ohm characteristic impedance.

The tests were conducted on a .020" thick alumina substrate suspended 0.15" above RF absorber. The gold metalization was 10 um thick, and the ground planes were not strapped together with any sort of bridge. These dimensions allowed scaling the 0 to 50 GHz results to a .010" thick substrate, with W and G half the size listed in Table 1, over the 0 to 100 GHz range. This also implied that no moding would take place, based on the monotonic nature of the data.

From these results the CPW probe boards were designed for primarily low conductor loss, since the radiation loss was no longer viewed as a major concern. At the probe tip the gaps and signal line width of the CPW line are reduced through a tapered region to give the required separation of the nickel fingers to match the DUT pad dimensions. To minimize radiation off the probe tip, this taper should not present any abrupt changes in transmission line field pattern or characteristic impedance. Excess radiation can couple to another probe tip during multi-port measurements. This can perturb data, particularly where low signal levels are involved, such as S_{12} in FET measurements.

IV. FUNCTIONAL PROBE DATA

Figure 7 illustrates the construction techniques employed for an actual probe. The probe block is split into upper and lower halves as shown. An insulating layer is placed between the two halves to provide dc isolation. Quarter wavelength RF chokes generate a virtual ground where the waveguide interior surface is split to minimize RF losses.

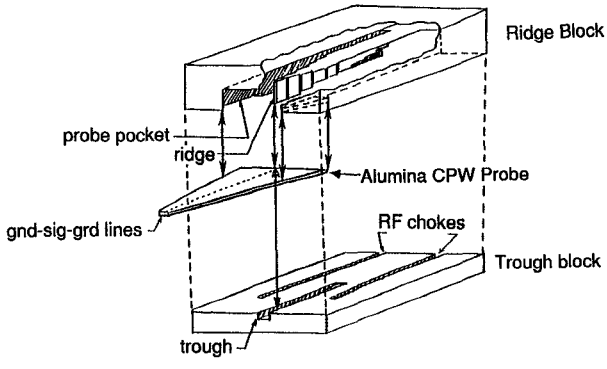

Figure 7. Exploded view of the waveguide input wafer probe

The alumina probe board is captured in a pocket that is machined into the upper block. The probe board is oriented such that the metalized ground-signal-ground lines are facing down, since this is the surface that must contact the wafer. A bond ribbon joins the signal line (shown by the dotted line) to the ridge after the probe is situated in the upper block. When the lower block is joined to the upper block the probe board is clamped into place. This clamping also brings the ground metalization of the probe board into electrical contact with the lower block. The end result is that the signal line and ground lines are electrically isolated and may be biased by applying a voltage to the upper and lower block halves respectively. In the event of probe board damage, the two halves may be separated and a new probe board installed.

The performance of an actual W-band wafer probe is shown in Figure 8, where S_{21}, S_{11}, and S_{22} versus frequency are shown. Port 1 is the waveguide input, and port 2 is the tip of the probe board. The insertion loss is typically about 3.5 dB across the band, with a worst case of 4.2 dB at 110 GHz. The return loss is typically better than 13 dB for both ports, with a worst case of 13.2 and 11.0 dB for ports 1 and 2 respectively, providing a good 50-ohm match to the DUT. Experience has shown that this level of insertion loss and return loss is sufficient for almost all corrected VNA applications. Knowing that the transition has 0.7-0.8 dB loss implies that the CPW board with taper section and nickel fingers has typically 2-3 dB insertion loss.

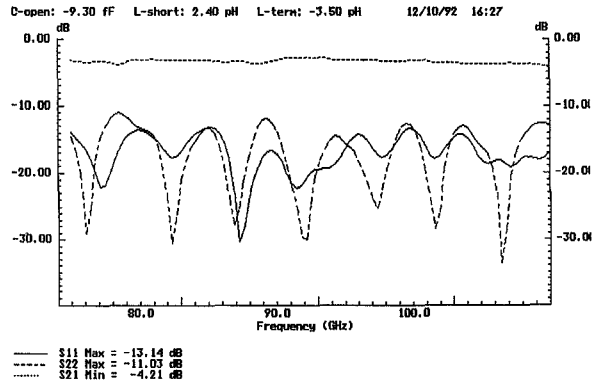

Figure 8. Insertion loss and return loss for the W-band probe.

One performance check for wafer probes is to perform a calibration at the probe tip and then measure S_{11} for an open transmission line. Figure 9 shows the data for a 40 pS long CPW line printed on alumina. S_{11} spirals inwards with increasing frequency due to skin effect losses in the line, as expected. The important observation is the lack of any perturbations in the trace due to spurious modes in the probe. This is also illustration of the correctability of the probe.

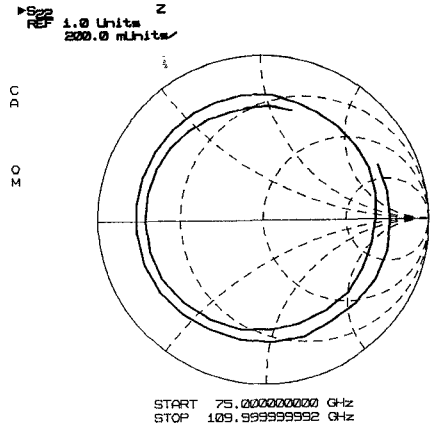

Figure 9. Open stub verification measurement, 40 ps CPW line.

A pair of W-band probes are shown on a wafer probing station in Figure 10. Note the bias cables connected to the side of the probes, which allows testing of active devices requiring bias at the probe tip. To test the crosstalk between the probes a two port calibration was first performed, and then the probes were adjusted to position the probe tips 0.004 inches apart in air and S_{21} was measured. This separation is chosen since this is a typical distance between probe tips during calibration.

The results are shown in Figure 11, where the worst case crosstalk is observed to be -43.6 dB at 105 GHz. Minimizing crosstalk between probes is critical for maintaining two-port on-wafer measurement integrity. This error is troublesome for most two port calibrations, where the isolation between the probes is assumed to be ideal [4]. Empirical studies have demonstrated that calibration integrity requires that probe crosstalk be less than -40 dB. These probes meet this requirement for accurate calibration.

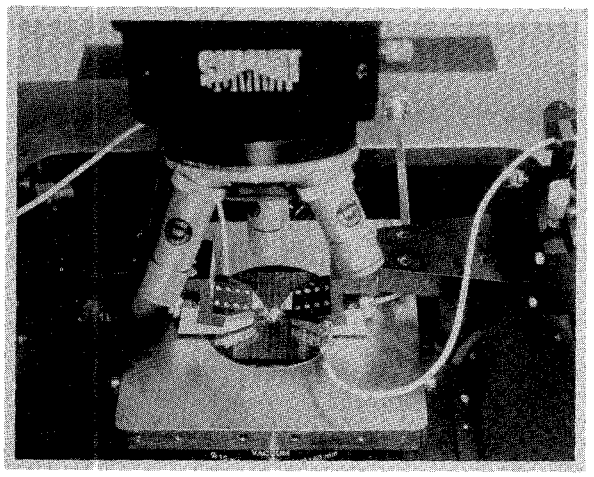

Figure 10. Pair of W-band probe in use.

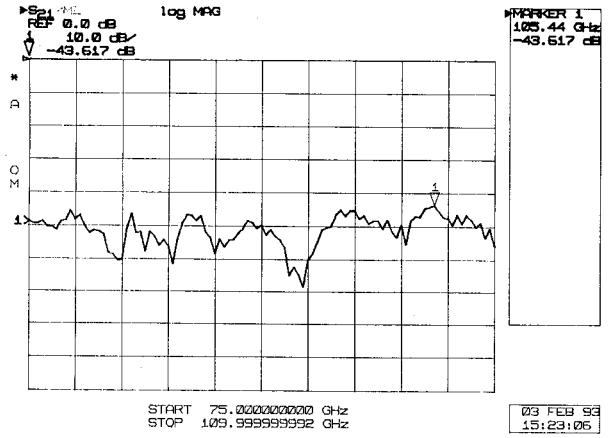

Figure 11. Crosstalk between two 100µm pitch probes, .004" separation.

V. HEMT DATA

With the W-band probes in place, active device measurements were performed on a psuedomorphic-HEMT (P-HEMT) and a 0.1x50 um passivated indium-phosphide HEMT. The forward (S_{21}) and reverse (S_{12}) gain for the P-HEMT is shown in Figure 12. In Figure 13, S_{11} and S_{22} for the InP HEMT are shown. Studies were conducted that indicate that the probes provide a sufficient match out of band to prevent any oscillation.

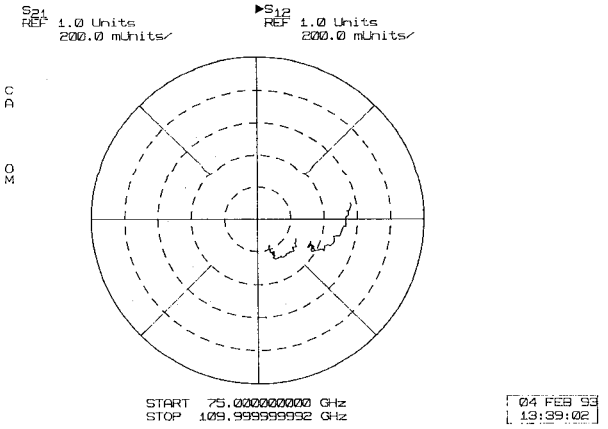

Figure 11. TRW InP HEMT Vgs = 0V, Vds = 2V, Ids = 6.2 mA.

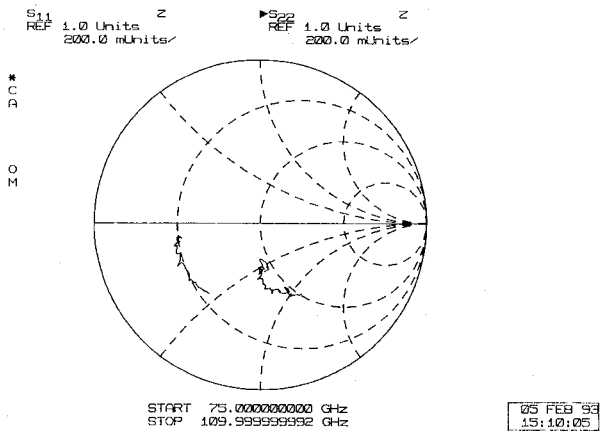

Figure 12. Hughes Research Lab InP HEMT 0.1x50µm passivated. V_D = 1.0V, V_G = 0V, I_D = 10.4 mA

VI. CONCLUSIONS

A W-band wafer probe was successfully designed and built. Typical insertion loss and return loss figures were 3.5 dB and better than 13 dB, respectively. Losses were minimized in the CPW probe board by attention to conductor loss and taper design, in addition the transition from rectangular waveguide to ridge-trough waveguide achieved less than 1 dB insertion loss. A crosstalk figure of better than -43 dB was achieved which is important for accurate calibrations. These performance specifications allowed measured data to be corrected by a VNA for some W-band HEMT devices.

VII. ACKNOWLEDGMENTS

This work was sponsored by the DARPA Phase III MIMIC program under the Department of the Army.
Thanks to Jeff Williams, Bernie Duman, Gerry Benedict, Eric Strid, John Pence, Dan d'Almeida, and Sally Lauer for their help in many different phases of the program.
The author is also grateful to Shin Chen and Ken Yano at TRW (Redondo Beach, CA) for the P-HEMTs, and Hughes Research Labs (Malibu, CA) for the InP HEMTs.

VIII. REFERENCES

[1] Cohen, E. D., 'The U.S. MIMIC Program-Status and Expectations," Applied Microwave Mag., Vol. 1, No.3, Nov/Dec, 1989, pp. 14-26.

[2] E. M. Godshalk, "A V-Band Wafer Probe Using Ridge-Trough Waveguide," IEEE Trans. Microwave Theory Tech., Vol. MTT-39, pp. 2218-2228, Dec. 1991.

[3] M. Riaziat, R. Majidi-Ahy, and I. J. Feng, "Propagation Modes and Dispersion Characteristics of Coplanar Waveguides," IEEE Trans. Microwave Theory Tech., Vol. MTT-38,.pp. 245-251, March 1990.

[4] A. Davidson, K Jones, and E. Strid, "LRM and LRRM with Automatic Determination of Load Inductance," 36th ARFTG Conf. Dig. (Monterey, CA), pp. 57-62, Nov. 1990.